RF LOSSES IN 1.3 GHz CRYOMODULE OF THE LCLS-II SUPERCONDUCTING CW LINAC*

A. Saini†, A. Lunin, N. Solyak, A. Sukhanov, V. Yakovlev, Fermilab, Batavia, USA

Abstract

The Linac Coherent Light Source (LCLS) is an x-ray free electron laser facility. The proposed upgrade of the LCLS facility is based on construction of a new 4 GeV superconducting (SC) linac that will operate in continuous wave (CW) mode. The major infrastructure investments and the operating cost of a SC CW linac are outlined by its cryogenic requirements. Thus, a detail understanding of RF losses in the cryogenic environment is critical for the entire project. In this paper we review RF losses in a 1.3 GHz accelerating cryomodule of the LCLS-II linac. RF losses due to various sources such untrapped higher order modes (HOMs), resonant losses etc. are addressed and presented here.

INTRODUCTION

The Linac Coherent Light Source -II (LCLS–II) [1] is a proposed fourth generation x-ray light source facility under construction at SLAC, California. The LCLS-II is primarily based on construction of a new 4 GeV SC RF linear accelerator (linac) that would operate in the CW regime (see Fig. 1).

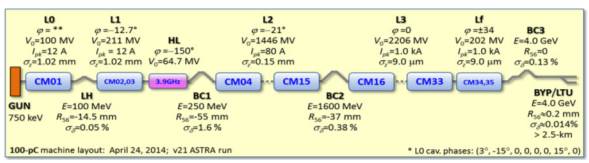

Figure 1: Layout of the LCLS-II SC linac.

The LCLS-II SC linac is segment into several sections which are named as L0, L1, HL, L2, L3 and Lf. All the sections except L1 and HL are separated to each other by intermediate warm sections which are designed for the specific purposes such as laser heating, diagnostic and bunch compressions. Excluding HL, all sections are composed of 9-cell 1.3 GHz SC TESLA like cavities [2]. HL section consists of 9-cell, 3.9 GHz SC cavities [3]. Number of elements and their nominal operational RF parameters in each section are summarized in Table 1 and a detailed description of the LCLS-II SC linac is presented elsewhere [4]. The cryogenic efficiency is significantly lower at operating temperature of 2 K [5]. Thus, operation of the SC linac in CW mode keeps a stringent tolerance on the cryogenic load of the machine. As, one can observe from Table 1 that major portion of the LCLS-II SC linac is comprised of the 1.3 GHz cryomodules and therefore, cryogenic budget of the facility is largely outlined by the cryogenic loads in a 1.3 GHz cryomodule. In this paper, we discuss and present contribution of different sources that result in the dynamic RF losses at the operating temperature of 2 K in a 1.3 GHz cryomodule in the LCLS-II SC linac.

Table 1: Configuration of Each Section in LCLS-II Linac

	Phase (deg)	Gradient (MV/m)	No. of CM's	Avail. cavities
L0	~0	16.3	1	8
L1	-12.7	13.6	2	16
HL	-150	12.5	2	16
L2	-21	15.5	12	96
L3	0	15.7	18	144
Lf	+/-34	15.7	2	18

1.3 GHZ CRYOMDOULE

Figure 2 shows a schematic of 1.3 GHz cryomodule. It accommodates eight cavities, a magnet package that includes a quadrupole magnet, a beam position monitor (BPM) and a dipole corrector and, a beam line absorber at the end.

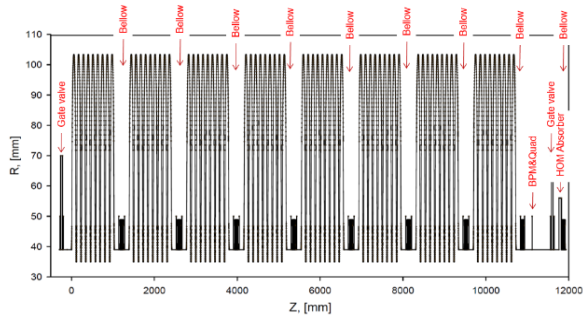

Figure 2: 2D view of a 1.3 GHz cryomodule for the LCLS-II SC linac.

Operating Mode RF Loss in Cavity

The major contribution to the dynamic RF losses in a cryomodule comes from dissipation of the operating mode fields on surface of the SC cavity. Power dissipated (P_d) on surface of a SC cavity is estimated as:

$$P_d = \frac{(E_{acc} L_{ef})^2}{\left(\frac{R}{Q}\right) Q_0}; \quad (1)$$

where E_{acc} is accelerating gradient, L_{ef} is cavity effective length and Q_0 is unloaded quality factor. For the 1.3 GHz,

* Work supported in part by Fermi Research Alliance, LLC under USA DOE Contract No. DE-AC02-07CH11359, DOE Contract No. DE-AC02-76SF00515 and the LCLS-II Project.
† asaini@fnal.gov

9-cell cavity, L_{ef} and R/Q are 1.038 m and 1012 Ω respectively. In the LCLS-II linac, cavities are spaced [6] to be operated with $Q_0 = 2.7 \times 10^{10}$ at $E_{acc} = 16 MV/m$. Using these values, estimated operating mode RF loss per cavity is about 10.1 W.

Untrapped Wake Losses in 1.3 GHz Cryomodule

When beam is traversed through the cryomodule, it radiates its wake energy into the higher order modes (HOMs). Primary source of excitation of those modes in the LCLS-II linac is irises in the nine-cell cavity. However, interconnecting cavity bellows and beam pipe transitions also contribute in this process. A frequency range of excited modes can be approximated as:

$$\omega \approx \frac{c}{\sigma_z}; \tag{2}$$

where c is velocity of light and σ_z is bunch length. In the LCLS-II linac, bunch length can be as short as *25* μm and therefore, spectrum of HOMs frequency extends up to tera-hertz. HOMs power deposited by beam is given as:

$$P_{HOM} = Q_b^2 f_{rep} \kappa \ ; \tag{3}$$

where Q_b is bunch charge, f_{rep} is bunch repetition frequency and κ is loss factor. A detailed analysis presented elsewhere [7] showed that maximum HOMs power deposited in a 1.3 GHz LCLS-II cryomodule is 13.8 W that corresponds to bunch charge of 300 pC, bunch repetition rate of 1 MHz and loss factor of 154 V/pC/CM. Loss factor is estimated for bunch length of 25 μm. In order to estimate fraction of HOMs power dissipating at 2 K in the cryomodule, one can express the total HOMs power deposited as sum of two parts i.e.,

$$P_{total} = \int_0^{\omega_c} \frac{dP}{d\omega} d\omega + \int_{\omega_c}^{\omega} \frac{dP}{d\omega} d\omega; \tag{4}$$

where first term is comprised of power below the cut-off frequency (ω_c) and, this power is effectively extracted out from the operating environment using HOMs couplers. The second term in Eq. (4) corresponds to HOMs that have frequencies above cut-off frequency. These modes can propagates freely in the linac and make multiple reflections to the beam line elements before they are completely absorbed. In this paper we will call them propagating or untrapped modes. One can evaluate HOMs power spectrum using the following equation:

$$\frac{dP}{d\omega} = Q_b^2 f_{rep} \, Z_{\|}(w) e^{-\left(\frac{\omega \sigma_z}{c}\right)^2}; \tag{5}$$

where $Z_{||}$ is longitudinal wake impedance estimated as:

$$Z_{\|} = \frac{1}{\pi c} \mathrm{Re}\left(\int_0^{\infty} w_{\|}^0(s) e^{\frac{-i\omega s}{c}} ds \right) \tag{6}$$

$w_{||}$ is wake function. Figures 3 and 4 show differential and integrated HOMs power spectrum in a 1.3 GHz and 3.9 GHz cryomodule of the LCLS-II linac. Integrated HOMs power above cut-off frequency is 12.8 W and 9.5 W for 1.3 GHz and 3.9 GHz cryomodule respectively. It is worth to mention here that HOMs power spectrum of the 3.9 GHz cryomodule is presented just for the completeness and a detailed discussion of the untrapped wake loss in the 3.9 GHz cryomodule is presented in this reference [8].

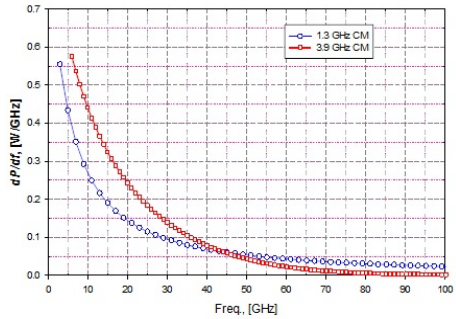

Figure 3: Differential power spectrum in a 1.3 GHz (blue) and 3.9 GHz (red) cryomodule of the LCLS-II SC linac.

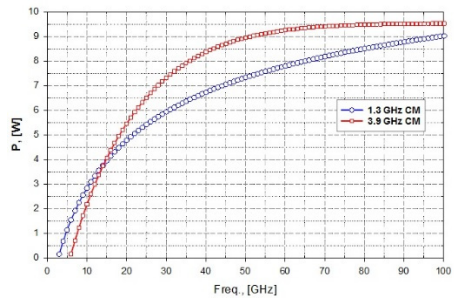

Figure 4: Integrated HOMs power spectrum in a 1.3 GHz (blue) and 3.9 GHz (red) cryomodule of the LCLS-II SC linac.

Because, frequency spectrum of the untrapped modes spread over tera-hertz range, estimation of distribution of their power dissipation in a cryomodule using the standard numerical methods is unfeasible. Thus, a diffusion model is developed which is based on the assumption that the untrapped HOMs can be treated as the photon gas distributed uniformly in the cryomodule. It is also assumed that untrapped HOMs dissipate all their power inside a cryomodule and therefore, no power leakage is anticipated in this model. This assumption is reasonably valid in presence of the long cryo-string (as in L2 and L3) where power leaking out from a cryomodule is equal to power coming in from its adjacent cryomodules in a steady state. According to the diffusion model, power absorption is proportional to the surface impedance and surface area of elements. Thus, the beamline elements can be grouped by type, for each of them the power absorption is characterized by their absorption coefficient given as:

$$I_i^{abs}(\omega) \sim n_i S_i \frac{dP(\omega)}{d\omega} \mathrm{Re}(Z_i(\omega)) d\omega; \tag{7}$$

where S_i is surface area of i^{th} type element (such as cavity, bellows, beam pipe etc.), n corresponds to number of i^{th} type element in a cryomodule and $Re(Z_i(\omega))$ is real part of the impedance at angular frequency of ω. The beam line absorber (BLA) in the LCLS-II linac is made from STL-150D aluminium nitride ceramic. The loss tangent and real part of the relative electrical permittivity for this

ISBN 978-3-95450-169-4

material are > 0.4 and ξ'_r <30. Figure 5 shows variation in the surface impedances of elements in the cryomodule with a wide range of frequency.

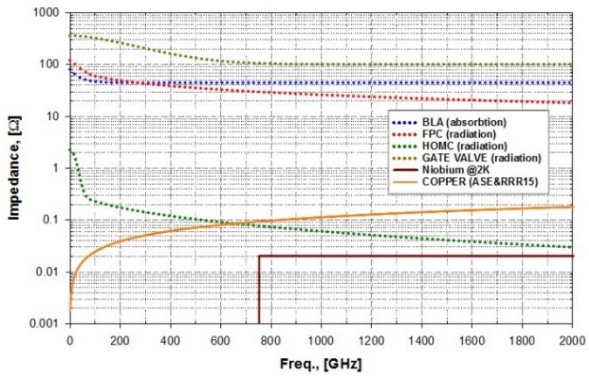

Figure 5: Variation in impedances of elements with frequency. FPC and HOMC correspond to fundamental power coupler and HOMs coupler respectively.

Using Eq. (7), dependence of surface impedance on frequency and HOMs differential power spectrum, one can estimate dissipation of untrapped HOMs power in a group of particular type of the element from equation shown below

$$P_i = \int_{\omega_c}^{\infty} \frac{dP}{d\omega} \frac{I_i^{abs}(\omega)}{\sum I_i^{abs}(\omega)} d\omega \qquad (8)$$

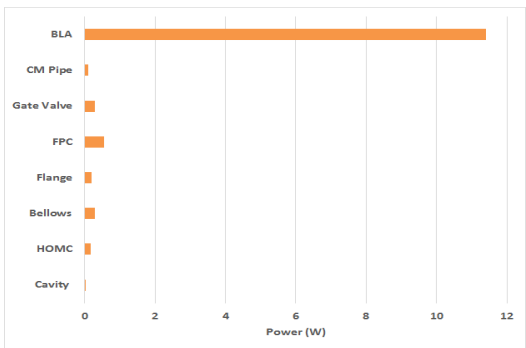

Figure 6: Distribution of untrapped HOMs power in the 1.3 GHz LCLS-II cryomodule.

Figure 6 shows distribution of the untrapped-HOM power in the 1.3GHz LCLS-II cryomodule. It can be observed that most of the power is deposited to the beam line absorber placed outside the operating temperature of 2K and only a small fraction (less than a Watt) out of 12.8 W is dissipated at 2K which is distributed among different elements (such as cavity, flanges, bellows). A thorough analysis is presented in [9].

RF Losses in Bellows

In the cryomodule two successive cavities are connected to each other through a stainless steel bellows (as shown in Fig. 2) having an inner copper coating of 15 μm +/- 5 μm. In some cases, propagating modes are reflected from ends of cavities and form a standing wave in the interconnecting cavity beam pipe, and therefore, are trapped there. Figure 7 shows a scenario when a mode is trapped in the interconnecting cavity beam pipe. Resulting RF loss can be estimated as:

$$P_{bt} = I^2 \left(\frac{R}{Q}\right) Q_{ext} \qquad (9)$$

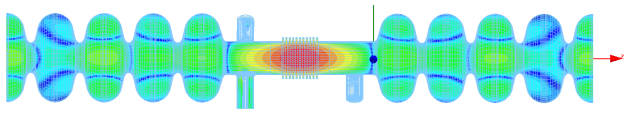

Figure 7: Trapped mode in interconnecting cavity beam pipe.

Beam current I of 0.3mA, $(R/Q) = 10\Omega$ and $Q_{ext} = 10^5$ result in a maximum beam loss of 0.1W. Furthermore, passing modes also result in the incoherent RF losses that can be estimated using:

$$P_{bln} = \sum_i \kappa_i Q^2 f \qquad (10)$$

For bunch charge of 300 pC and repetition frequency of 1 MHz, RF loss due to passing modes (summed over all modes up to 10 GHz) are less than 10 mW. Additional to HOMs generated RF losses, decay of operating mode field into the beam pipe also results in a RF loss at the bellows. For the design operating gradient of 16 MV/m, RF loss due to operating field leaking from cavities at both sides of bellows is approximately 2 mW. RF loss at flanges due to operating mode field is about 100 mW.

Resonance Excitation of HOMs

A detailed study has been performed and presented elsewhere [10] to analyse possibility of resonance excitation and corresponding RF losses in the LCLS-II SC linac. Total power dissipated on the surface of the cavity due to HOMs excited by beam harmonics is given as:

$$P_c = \sum_p \sum_n \frac{\omega_p^4}{(\omega_n^2 - \omega_p^2)^2 + \left(\frac{\omega_n \omega_p}{(Q_L)_p}\right)^2} \frac{I_n^2}{4} \left(\frac{R}{Q}\right)_p \left(\frac{1}{Q_0}\right)_p \qquad (11)$$

where I_n and ω_n are n^{th} beam harmonic current and angular frequency respectively; ω_p , $(Q_L)_p$ are angular frequency and loaded quality factor of the p^{th} mode. It is evaluated that even for the worst scenario i.e. $Q_L = 10^7$ and including HOMs up to 10 GHz, median RF loss (50 % probability) in a SC cavity is below 10 mW.

SUMMARY

A large portion of the LCLS-II SC linac is comprised of 1.3 GHz cryomdoules. A detailed study has been performed to determine RF losses at operating temperature of 2K in the 1.3 GHz cryomdoule. Most of the major sources that contribute to cryogenic load were discussed. The cryogenic capacity of the LCLS-II cryogenic system at 2 K is 8 kW while maximum total RF losses (static and dynamic) even after including uncertainty factors are expected to be less than 4 kW [11].

REFERENCES

[1] T. O. Raubenheimer, "LCLS-II: Status of the CW X-ray FEL Update to the LCLS Facility," *in Proc. FEL'15*, Daejeon, Korea, 2015, paper WEP014, pp. 618-624.

[2] B. Aune, *et al*., "Superconducting TESLA cavities," *Phys. Rev. ST Accel. Beams*, vol. 3, p. 092001-1-25, 2000.

[3] E. Harms, *et al*., "Status of 3.9 GHz Superconducting RF cavity technology at Fermilab," in *Proc. LINAC'08*, British Columbia, Canada, 2008, paper THP028, pp. 845-847.

[4] P. Emma, *et al*., "Linear Accelerator Design for the LCLS-II FEL facility," in *Proc. FEL'14,* Basel, 2014, paper THP025, pp. 743-747

[5] A. Saini, *et al*., "Estimation of Cryogenic Heat Loads in Cryomodule due to Thermal Radiation," in *Proc. IPAC2015*, pp. 3338-3341.

[6] T. Raubenheimer, "SCRF 1.3 GHz Cryomodule," SLAC, California, USA, Rep. LCLSII-4.1-PR-0148-R0, April 2014.

[7] K. Bane, *et al*., "Some Wakefield Effects in the Superconducting RF Cavities of LCLS-II," SLAC, California, USA, Rep. LCLS-II TN-13-04.

[8] A. Lunin, *et al*., "Generation and Absorption of the Untrapped Wakefield Radiation in the 3.9 GHz LCLS-II Cryomodule," SLAC, California, USA, Rep. LCLS-II TN-16-06.

[9] K. Bane, *et al*., "Distribution of Heating from Untrapped HOM Radiation in the LCLS-II Cryomodule," in Science Direct, Physics Proceida (2015) 000-000.

[10] A. Sukhanov, *et al*., "Resonant excitation of high order modes in superconducting RF cavities of LCLS II linac," SLAC, California, USA, Rep. LCLS-II TN-15-06.

[11] T. Peterson, *et al*., "Cryogenic Heat Load," SLAC, California, USA, Rep. LCLSII-4.5-EN-0179-R2.

ISBN 978-3-95450-169-4